

Transmission and reflection of charge density waves in a quantum Hall edge controlled by a metal gate

Masahiro Matsuura,¹ Takaaki Mano,² Takeshi Noda,² Naokazu Shibata,¹ Masahiro Hotta,¹ and Go Yusa^{1, a)}

¹⁾Department of Physics, Tohoku University, Sendai 980-8578, Japan

²⁾National Institute for Materials Science, Tsukuba, Ibaraki 305-0047, Japan

(Dated: 18 November 2021)

Quantum energy teleportation (QET) is a proposed protocol related to the quantum vacuum. The edge channels in a quantum Hall system is well suited for the experimental verification of QET. For this purpose, we examine a charge density wave excited and detected by capacitively coupled front gate electrodes. We observe the waveform of the charge density wave, which is proportional to the time derivative of the applied square voltage wave. Further, we study the transmission and reflection behaviors of the charge density wave by applying a voltage to another front gate electrode to control the path of the edge state. We show that the threshold voltages where the dominant direction is switched in either transmission or reflection for dense and sparse waves are different from the threshold voltage where the current stops flowing in an equilibrium state.

The physics of the quantum vacuum and its fluctuations (zero-point fluctuations) have attracted considerable attention in various fields of modern physics¹. Quantum energy teleportation (QET) is one quantum-vacuum-related protocol^{2,3}. By this protocol, the local zero-point energy is extracted from a remote place by only sending classical information, which does not carry energy but contains how to extract energy from the local vacuum. In order to verify this quantum protocol by experiment, a quantum Hall (QH) system has been theoretically suggested to be the best suited physical system^{4,5}. The QH states consist of two regions—bulk and edge. When a strong perpendicular magnetic field is applied to the two-dimensional (2D) electrons, the orbital degree of freedom of the electrons in the bulk region is quantized and does not contribute to the transport. However, electrons in the edge region can flow without backscattering, leading to a zero longitudinal resistance⁶. Using intriguing properties of edge channels and the charge density waves propagating along them, pioneering experiments have been performed^{7–10,12}. To perform the QET protocol, excitation and detection through capacitively coupled gate electrodes are required^{4,5}. In most experiments, however, the charge density wave in the edge channel has been measured through ohmic contacts as a current flow^{10,12}. The study of detection by a capacitively coupled contact is very limited⁸. In this paper, we establish a detection scheme for measuring the charge density wave through a capacitively coupled gate electrode as a key ingredient for experimental verification of the QET protocol.

We used a GaAs/AlGaAs single heterostructure as a 2D system. The as-grown electron density and mobility at 45 mK are $2.3 \times 10^{11} \text{ cm}^{-2}$ and $1.3 \times 10^6 \text{ cm}^2/(\text{Vs})$, respectively. Using photolithography and electron-beam lithography, we fabricated the device shown in Fig. 1. The center gate connected to a direct current (dc) voltage

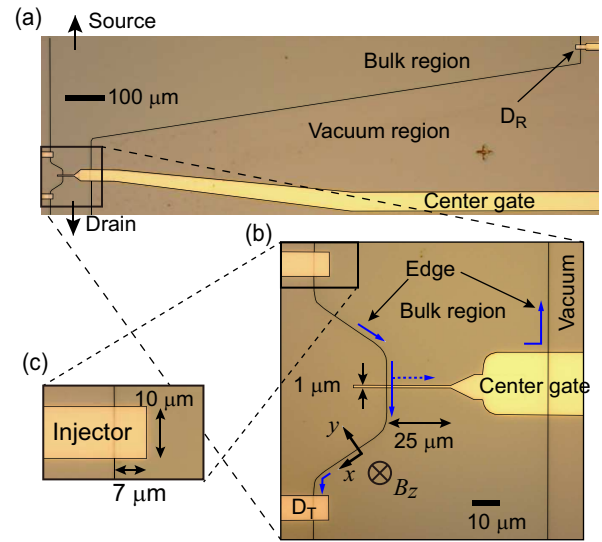


FIG. 1. (a) Optical microscope images of our device. (b) Close-up of the center region. (c) Close-up of the injector, which is used to apply a voltage and excite charge density waves in the edge channel. Detectors D_T and D_R are used to measure the density wave. By applying a negative center gate voltage, V_C , the two-dimensional electrons beneath the center gate can be depleted, and the paths of the wave packets can be switched between detectors D_T and D_R . The direction of the edge channel is indicated by the blue arrows. The contours of the mesa and gate electrodes are outlined for clarity.

source can deplete the electrons under the gate with the application of a negative center gate voltage V_C . Thus, a change in V_C can alter the path of the edge channel from the injector to either of the two detectors, D_T or D_R . We define transmission as the path along which a charge density wave is transmitted through the center gate and reflection as the path along which a charge density wave is reflected by the center gate. The injector, D_T , and D_R are front gate electrodes made with 20- and 80-nm-thick Ti and Au. They are capacitively coupled with

^{a)}Electronic mail: yusa@tohoku.ac.jp

the edge channels in an equivalent manner. Moreover, electron-beam lithography was used to process them and the narrow region of the center gate. A voltage signal from a function generator is transmitted to the injector to excite a charge density wave, which propagates along the edge channel in the directions indicated by blue arrows in Fig. 1(b). D_T and D_R are connected to an oscilloscope at room temperature through a coaxial cable. The voltage signals measured by the 200-MHz bandwidth oscilloscope from D_T and D_R are V_T and V_R , respectively. No filters or amplifiers are introduced between the detectors and the oscilloscope. The experiment was performed with a magnetic field $B_z = 9.5$ T applied along the z axis perpendicular to the 2D plane. In this condition, the Landau-level filling factor ν is unity. The typical base temperature is ~ 45 mK.

First, we tested the behavior of the center gate. We applied an alternating voltage with an amplitude $V_{SD} = 10$ mV oscillating at 13 Hz between the source and the drain, i.e., two ohmic contacts. The current between them, I_{SD} , was measured by the lock-in technique as a function of V_C . By decreasing V_C , I_{SD} decreases at $V_C \sim -0.5$ V because the electrons under the center gate are depleted, and the electron flow between the source and the drain is hampered. Below $V_C < \sim -0.6$ V, I_{SD} becomes ~ 0 , indicating that the bulk regions connected to the source and drain are separated from each other by the depleted region under the center gate.

In order to excite a charge density wave, we used a square voltage wave. A typical input voltage V_{in} was measured by the oscilloscope by direct connection to a signal generator. The typical rise and fall times of the square wave are a few nanoseconds. The waveform has slight under- and overshoots [Fig. 2(b)]. Thus, the time derivative dV_{in}/dt of this square wave has positive and negative peaks corresponding to the rising and falling of the square wave, respectively, and has a small negative peak right after the sharp positive peak at $t \sim 1$ ns in Fig. 2(c), originating from the overshoot of the square wave. We discuss this waveform of V_{in} and dV_{in}/dt later in relation to the waveforms observed at D_T and D_R .

We injected square waves with amplitudes of 0.5 V and duration times of 5 ns. With these square waves, a density wave is excited in the edge channel and propagates along the edge, and we measure the waveforms at D_T and D_R . We repeatedly performed single-shot measurements 6000 times, and the averaged data are displayed in Fig. 3. When V_C is close to ~ 0 V, a voltage signal was only detected at D_T [Fig. 3(a)], and no signal was detected at D_R [Fig. 3(c)]. All waves are transmitted through the center gate because the edge channel is connected from the injector to D_T but not to D_R . By decreasing V_C , the amplitude of V_T tends to become weak [Fig. 3(b)], whereas that of V_R becomes large [Fig. 3(d)], suggesting that some part of the charge density wave starts to propagate along the edge formed by the center gate to reach the right-hand side of the sample edge, which is connected to D_R . In other words, some part of

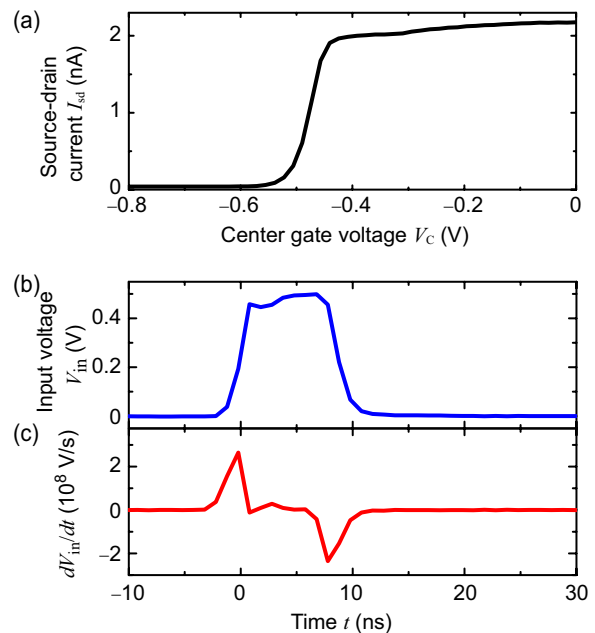


FIG. 2. (a) Source–drain current I_{sd} dependence as a function of the center gate voltage V_C at $\nu = 1$, $B = 9.5$ T, and $T = 40$ mK. (b) A typical waveform of the input voltage V_{in} for exciting a charge density wave. The waveform was measured by connecting a signal generator directly to an oscilloscope. (c) Time derivative dV_{in}/dt of the waveform of Fig. 2(b). The time origin is arbitrary.

the charge density wave is reflected by the center gate. At $V_C = -0.8$ V, no signal was detected at D_T because the center gate is closed and all charge density waves are reflected by the center gate to D_R .

The observed waveforms of V_T and V_R are not analogous to the waveform of the applied voltage V_{in} [Fig. 2(b)] but to that of dV_{in}/dt [Fig. 2(c)]. When a square voltage wave is applied to the injector, the electric field, i.e., the slope of the local confinement potential $U(t)$, becomes small. Since the velocity $v(t)$ of the electrons in the edge channel is $v(t) = \frac{1}{|e|B} \frac{dU(t)}{dy}$, $v(t)$ becomes temporarily small during the rise time of the square pulse, which creates a local dense region in the charge density wave. When the applied voltage becomes constant, i.e., during the flat time region of the square pulse, $v(t)$ is also constant over time, and the charge density is constant. Thus, no charge density wave is created. During the fall time, a local sparse region is created because $v(t)$ temporarily becomes large. Therefore, the waveform of the charge density wave is proportional to $dv(t)/dt$. Note that since the QH state is incompressible, the electron density in the bulk is constant. Thus, the change in the charge density corresponds to the deformation of the edge⁶. The dense and sparse regions correspond to the convexity and concavity of the boundary. Since D_T and D_R are capacitively coupled to the edge channel, each waveform of V_T and V_R is proportional to the charge density wave.

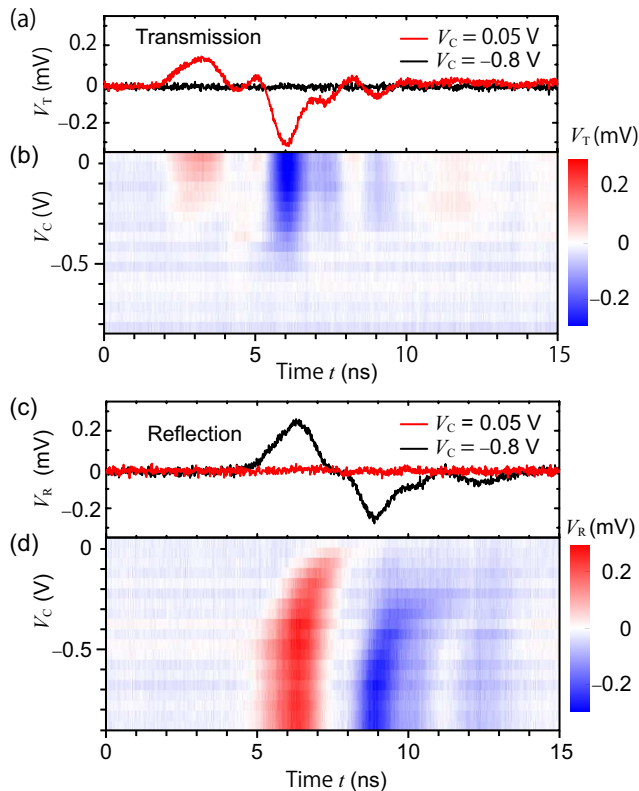


FIG. 3. (a) Waveforms of the voltage V_T obtained at D_T at $V_C = 0.05$ V (black) and -0.8 V (red) as a function of the time t . (b) V_C dependencies of the voltage waveforms obtained from D_T . (c) Waveforms of the voltage V_R obtained at D_R at $V_C = 0.05$ V (black) and -0.8 V (red) as a function of the time t . (d) Voltage waveforms obtained at D_R as a function of V_C . All data were obtained at $\nu = 1$, $B = 9.5$ T, and ~ 40 mK. The increment in V_C for Figs. 2(b) and 2(d) is 50 mV.

The V_C dependencies of the transmission and reflection of the dense and sparse waves are notable. The peak values of V_T and V_R for dense and sparse waves are plotted as a function of V_C in Fig. 4(a). For the dense wave (red), the transmission and reflection cross each other at $V_C \sim -0.07$ V. In contrast, for the sparse wave (blue), it requires a further negative voltage of $V_C \sim -0.36$ V for the transmission and reflection to cross each other. Note that the value of V_C at which I_{sd} sharply decreases is $V_C \sim -0.46$ V [Fig. 2(a)]. This may be because some electrons can be excited to higher Landau levels when the dense region is created by the rising part of the square wave. In contrast, the electrons in the sparse region cannot be excited because there are no states. In other words, the charge density waves are excited so strongly that the electron-hole symmetry is broken. This is consistent with the fact that the waveforms of the dense and sparse waves observed in reflection [the red line in Fig. 3(c)] are more symmetric with respect to the 0-mV line than those observed in transmission [the black line in Fig. 3(a)]. This may be because all of the electrons ex-

cited to the higher Landau levels can be easily relaxed by the center gate, which functions as a scattering center, for $V_C = -0.8$ V, and they do not contribute to the reflection signal. In contrast, for $V_C = 0.05$ V, the influence of the center gate is small, and the dense wave is broader than the sparse wave in transmission.

The time difference δt_{R-T} between the local maximum in V_T at $V_C = -0.05$ V [Fig. 3(a)] and that in V_R at $V_C = -0.8$ V [Fig. 3(c)] is ~ 3 ns and is equal to the difference in the arrival times of the charge density waves at D_T and D_R . Thus, $\delta t_{R-T} = l_C/v_C + (l_T - l_R)/v$, where l_T , l_R , l_C , and v_C are the edge channel length between the center gate to D_T , that between the center gate to D_R , that along the center gate, and the velocity of the edge channel along the center gate, respectively. Here, $l_T = 65$ μm , $l_R = 1.3$ mm, and $l_C = 65$ μm . Since $l_R \gg l_T, l_C$ and the order $O(v) \sim O(v_C)$, δt_{R-T} can be approximated by l_R/v , resulting in $O(v) \sim 4 \times 10^5$ m/s ($\sim 1.3 \times 10^{-3} c$, where c is the speed of light).

The local maximum and minimum in V_T appear at $t \sim 3$ and ~ 6 ns, independent of V_C [Fig. 3(b)], whereas those in V_R shift as a function of V_C for $V_C > \sim 0.4$ V

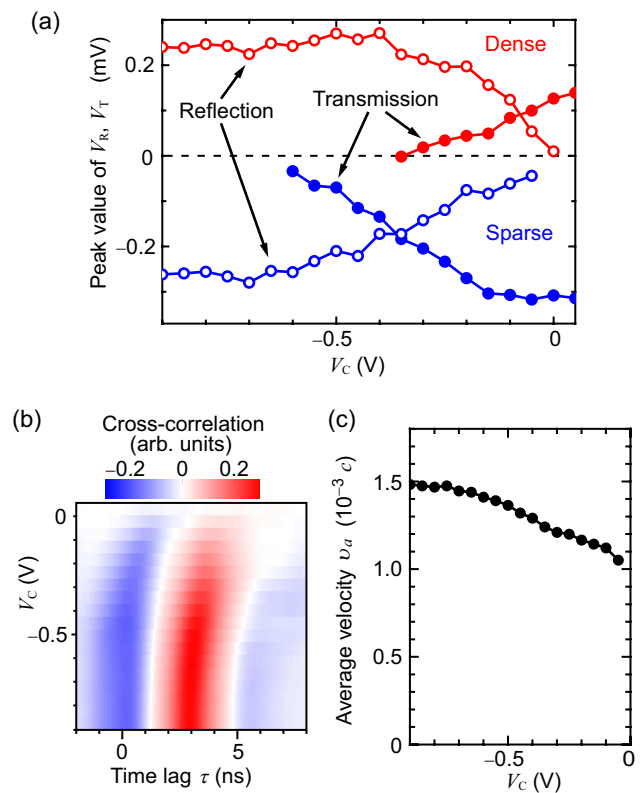


FIG. 4. (a) V_C dependence of the amplitude of the local minima (blue) and maxima (red) of V_R (open circles) and V_T (filled circles) in Figs. 3(b) and 3(d). (b) Cross-correlation of V_T at $V_C = -0.05$ V and V_R at each V_C as a function of the time lag τ . (c) Average velocity v_a of the charge density wave as a function of V_C in units of the speed of light in vacuum, $c \sim 3.00 \times 10^8$ m/s.

and remain constant for $V_C < \sim 0.4$ V [Fig. 3(d)]. This may be because the velocity changes when the charge density wave propagates along the center gate electrode, as reported earlier¹⁰. To obtain δt_{R-T} systematically, the cross-correlation of $V_T(t)$ at $V_C = -0.05$ V and $V_R(t)$ at each V_C , i.e., $\int V_T(t)V_R(\tau - t)dt$, is calculated as a function of V_C . Here, τ is the time lag. A strong positive correlation [the red region in Fig. 4(a)] appears near $\tau \sim 3$ ns, which corresponds to δt_{R-T} . The average velocity $v_{\text{avg}} = (l_C + l_2)/\delta t_{R-T}$ between the center gate and D_R is plotted as a function of V_C in Fig. 4(c). By decreasing V_C , v_{avg} gradually increases and becomes constant below $V_C < \sim -0.7$ V.

ACKNOWLEDGMENTS

The authors are grateful for discussions with T. Fujisawa, K. Kobayashi, T. Arakawa, J. N. Moore, R. Schützhold, and W. G. Unruh. This work was supported by the Asahi Glass Foundation;

MEXT/JSPS KAKENHI Grant Numbers JP 17H01037 and 16K05311(M.H.); and the “Nanotechnology Support Project” of MEXT.

- ¹P. W. Milonni, *The Quantum Vacuum* (Academic Press, 1994).
- ²M. Hotta, *Phys. Lett. A* **372**, 5671 (2008).
- ³M. Hotta, *J. Phys. A: Math. Theor.* **43**, 105305 (2010).
- ⁴G. Yusa, W. Izumida, and M. Hotta, *Phys. Rev. A* **84**, 032336 (2011).
- ⁵M. Hotta, J. Matsumoto, and G. Yusa, *Phys. Rev. A* **89**, 012311 (2014).
- ⁶D. Yoshioka, *The Quantum Hall Effect* (Springer, Berlin, 2002).
- ⁷S. J. Allen, H. L. Stormer, and J. C. M. Hwang, *Phys. Rev. B* **28**, 4875 (1983).
- ⁸R. C. Ashoori, H. L. Stormer, L. N. Pfeiffer, K. W. Baldwin, and K. West, *Phys. Rev. B* **45**, 3894 (1995).
- ⁹G. Fève, A. Mahe, J.-M. Berroir, T. Kontos, B. Plaçais, D. C. Glatli, A. Cavanna, B. Etienne, Y. Jin, *Science* **316**, 1169 (2007).
- ¹⁰H. Kamata, T. Ota, K. Muraki, and T. Fujisawa, *Phys. Rev. B* **81**, 085329 (2010).
- ¹¹Although we only discuss the average velocity of charge density waves in this paper, one should note that the change of the velocity of the edge channel along the center gate, v_C , appears to be much bigger than reported earlier.
- ¹²M. Hashisaka, N. Hiyama, T. Akiho, K. Muraki, and T. Fujisawa, *Nat. Phys.* doi:10.1038/nphys4062 (2017).